WARSAW UNIVERSITY OF TECHNOLOGY Index 351733
FACULTY OF CIVIL ENGINEERING
COMMITTEE FOR CIVIL AND WATER ENGINEERING
POLISH ACADEMY OF SCIENCES ISSN 1230-2945

DOI: 10.24425/ace.2024.151881

ARCHIVES OF CIVIL ENGINEERING

Vol. LXX ISSUE 4 2024

pp. 85 –98

Research paper

Application of the Rayleigh quotient method in the analysis of stability of straight elastic bars

Radosław Czubacki[1], Tomasz Lewiński[2]

Abstract: The paper deals with stability problems of straight elastic bars made of a homogenous isotropic material. The approach concerns both the bars of compact cross-sections and of thin-walled cross-sections, the transverse distortions being neglected. The stability analysis method developed for thin-walled bars in the paper: L. Zhang and G.S. Tong, "Flexural-torsional buckling of thin-walled beam members based on shell buckling theory", Thin-Walled Structures, vol. 42 (2004), pp. 1665–1687 is here extended to the bars whose deformations obey the assumptions of the Vlasov-like theory. The approach proposed makes it possible to assess the values of critical loads causing: axial forces, bending moments, transverse forces and torques, possibly simultaneously. The main task is to perform maximization of the relevant Rayleigh quotient; its form is given for all rational shapes of the bar's cross section. The paper shows how to assess critical axial buckling loads and lateral buckling loads of straight elastic bars made of a homogenous isotropic material.

Keywords: lateral-torsional buckling, stability, theory of bars, thin-walled bars

[1]PhD., Eng., Warsaw University of Technology, Faculty of Civil Engineering, Al. Armii Ludowej 16, 00-637 Warsaw, Poland, e-mail: radoslaw.czubacki@pw.edu.pl, ORCID: 0000-0001-6502-5864
[2]Prof., DSc., PhD., Eng., Warsaw University of Technology, Faculty of Civil Engineering, Al. Armii Ludowej 16, 00-637 Warsaw, Poland, e-mail: tomasz.lewinski@pw.edu.pl ORCID: 0000-0003-2299-2162

1. Introduction

The Vlasov theory of thin-walled straight bars of open cross sections has been recently extended to encompass deformation modelling of straight bars of arbitrary cross-sections, cf. Lewiński & Czarnecki [1]. This new method will be called a *Vlasov-like theory of bars*. The mathematical structure of the theory coincides with that of Vlasov's, while the sectional characteristics are computed by appropriate procedure reducing to solving three auxiliary elliptic problems posed on the bar's section domain. This makes it possible to set a framework for solving a vast family of static and stability problems including axial and lateral buckling of bars with admissible boundary conditions. The known solutions concerning thin-walled bars of open cross sections published in Gawęcki [2], Weiss and Giżejowski [3], Timoshenko & Gere [4], Trahair et al. [5], Petersen [6], Zhang and Tong [7–9] and Piotrowski and Szychowski [10–13] can now be extended towards bars of solid cross-sections of practically arbitrary geometry. It occurs that the Rayleigh quotient method appears to be a well-chosen tool to set and solve the main problems of stability of a single bar. The aim of the present paper is to put forward the details of this method, amending it with original concepts by Zhang & Tong [7–9] based on the Vlasov theory of bars of open profiles. The final expressions of the Rayleigh quotients turn out to be compatible with those found by Zhang & Tong [7–9] although based on different formulae of stress recovery in the bar treated as a spatial body. The paper puts forward new methods of solving the maximization problems corresponding to the Rayleigh method. The approach proposed is illustrated by examples concerning mono-symmetric and bisymmetric profiles.

2. A unified approach to stability of spatial elastic bodies

Consider a 3D elastic anisotropic body with moduli $C^{ijkl}(\boldsymbol{x})$; the body is supported on a certain part of the boundary (thus preventing from the rigid motions) and subject to the loads being proportional to a multiplier λ. Before achieving the state of the loss of stability of equilibrium the stresses $\lambda\sigma_o^{ij}(\boldsymbol{x})$ appear. The tensor fields $C^{ijkl}(\boldsymbol{x})$ and $\sigma_o^{ij}(\boldsymbol{x})$, given in the domain Ω occupied by the body in its initial configuration, are involved in the numerator and denominator of the Rayleigh quotient; its argument is the kinematically admissible vector field of displacements denoted by $\boldsymbol{v}$. According to the linear theory of stability, cf. Washizu [14] and Zhang & Tong [7–9], the critical value of the load multiplier λ is expressed by

(2.1)
$$\frac{1}{|\lambda_{\text{crit}}|} = \max_{\substack{v \text{ being} \\ \text{kinematically admissible}}} \left(\int_\Omega \sum_{i,j,k=1}^{3} \sigma_o^{ij} \frac{\partial v_k}{\partial x_i} \frac{\partial v_k}{\partial x_j} \mathrm{d}\Omega \right) \left(\int_\Omega \sum_{i,j,k,l=1}^{3} C^{ijkl} \frac{\partial v_i}{\partial x_j} \frac{\partial v_k}{\partial x_l} \mathrm{d}\Omega \right)^{-1}$$

Here x_i, $i = 1, 2, 3$ are coordinates of a Cartesian coordinate system parametrizing the domain of the body; v_i is the i th component of the virtual displacement field $\boldsymbol{v}$. The formula Eq. (2.1) is highly practical, since the kinematic boundary conditions are independent of the multiplier which is unknown. This property still holds within the 1D modelling, which is a crucial argument justifying using the Rayleigh quotient method in the analysis of stability of bars.

3. Stability of equilibrium of bars of arbitrary cross sections

To perform the stability analysis we express: the displacement fields as well as stress fields in Eq. (2.1) in terms of the fields (referred to the longitudinal axis) involved in the bar theory. Here we use the kinematic assumptions of the Vlasov-like theory (cf. Eqs (5.1–5.3) in Lewiński & Czarnecki [1]) omitting the last two terms in Eqs (5.1) and we use the formulae for stresses expressed in terms of the stress resultants according to Librescu & Song's theory, see Eqs (1.2.1–3) and (5.3.1) (without two last terms) and Eqs (5.3.2)–(5.3.4-6) in Lewiński & Czarnecki [1]. In the Vlasov-like bar theory all the fields are referred to the $x = x_1$ axis linking the shear centers S of coordinates $x_2 = y_s$, $x_3 = z_s$ on the plane x = const of the bar's transverse cross section. Within the *Vlasov-like theory* the bar is subjected to the axial and transverse loadings, the latter being applied along the line linking the shear centers. The intensities of distributed loadings applied in y and z directions are denoted by $q_y(x)$, $q_z(x)$, respectively. The deformation of the bar is described with using the displacements $u(x)$, $v(x)$, $w(x)$ of points along the line linking the shear centers and the field $\theta\,(x)$ representing the angle of twist along the x axis. This dimension reduction to a one-dimensional model leads to the expression for the elastic energy stored in the bar subject to bending and torsion, being the denominator in Eq. (2.1); it is given by Eq. (9.5) in the paper by Lewiński & Czarnecki [1]. On the other hand, the state of stress $\sigma_o^{ij}\,(x)$ within the bar can be expressed in terms of the axial force $N^o\,(x)$, bending moments $M_y^o\,(x)$, $M_z^o\,(x)$ transverse forces $T_y^o\,(x)$, $T_z^o\,(x)$, the bimoment $B^o\,(x)$ and the torsional moment $M^o\,(x)$. This leads to the Rayleigh quotient Eq. (2.1) in the form involving only the terms of the Vlasov-like theory. The maximization operation can be performed analytically, semi-analytically or numerically.

The dimension reduction process described above requires a special care if the load is applied not along the line linking the shear centers but is shifted in the y or z directions. The transverse load $q_z(x)$ may be applied to the points of the axis $(x,\, y_s,\, z_2)$ while the lateral load $q_y(x)$ – to the points of the axis $(x,\, y_1,\, z_s)$, see Fig. 1. These shifts affect the value of the work of the initial stresses forming the numerator in the quotient (2.1), which will be discussed in the sequel.

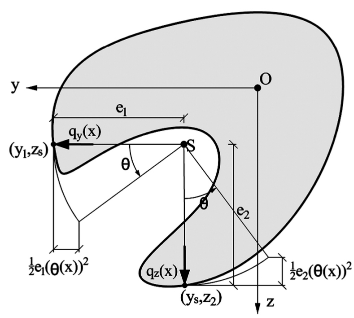

Fig. 1. Parametrization of the bar's cross section; y and z are principal axes; position of the centroid (O) and the shear center (S). Possible points of applications of the transverse and lateral loads are shown. When the section is rotated by the virtual angle θ, the points of applications of these loads displace along the lines of applications of the loads, hence an additional virtual work is created

4. The Rayleigh quotient method as a tool of solving the problems of stability of bars

As noted in Sections 2 and 3 the reduction of the dimensions: from the spatial to one-dimensional in the expression for the Rayleigh quotient (2.1) leads to the problem of the form

$$\frac{1}{|\lambda_{\text{crit}}|} = \max_{\substack{v,w,\theta \text{ being} \\ \text{kinematically admissible}}} \frac{W_0\,(v,w,\theta)}{W\,(v,w,\theta)} \tag{4.1}$$

where $W\,(v,w,\theta)$ stands for the elastic energy stored in the bar; it is given by the Eq. (9.5) in Lewiński & Czarnecki [1]; $v(x)$, $w(x)$ represent displacements along the axes y (lateral) and z (vertical) of points lying along the line $(x,\, y_s,\, z_s)$ linking the shear centers, while $\theta\,(x)$ represents the angle of twist (in the x direction).

Consider now the case of the transverse loads being applied at points along the axis linking the shear centers; this means that quantities e_1, e_2 (shown in Fig. 1) vanish. The quantity $W_0\,(v,w,\theta)$ standing for the work of initial stresses (the numerator of the quotient (2.1)) can be expressed by the terms of Vlasov-like theory as follows

$$W_0 = \frac{1}{2}\int_0^l \left[N^o\,(x)\,b_N\,(x) + M_y^o\,(x)\,b_y^M\,(x) + M_z^o\,(x)\,b_z^M\,(x) + B_x^0\,(x)\,b_\omega\,(x) + M^o\,(x)\,b_M\,(x) + T_z^o\,(x)\,b_z^T\,(x) + T_y^o\,(x)\,b_y^T\,(x)\right]\mathrm{d}x + \widetilde{W}_y + \widetilde{W}_z \tag{4.2}$$

where

$$\widetilde{W}_y = -\frac{a_z}{4}\int_0^l q_y\,(x)\,\theta^2\,(x)\mathrm{d}x, \qquad \widetilde{W}_z = -\frac{a_y}{4}\int_0^l q_z\,(x)\,\theta^2\,(x)\mathrm{d}x \tag{4.3}$$

and

$$\begin{aligned}
b_N\,(x) &= \left(\frac{\mathrm{d}w}{\mathrm{d}x}\right)^2 + \left(\frac{\mathrm{d}v}{\mathrm{d}x}\right)^2 + 2z_s\frac{\mathrm{d}v}{\mathrm{d}x}\frac{\mathrm{d}\theta}{\mathrm{d}x} - 2y_s\frac{\mathrm{d}w}{\mathrm{d}x}\frac{\mathrm{d}\theta}{\mathrm{d}x} + (r_0)^2\left(\frac{\mathrm{d}\theta}{\mathrm{d}x}\right)^2 \\
b_y^M\,(x) &= a_y\left(\frac{\mathrm{d}\theta}{\mathrm{d}x}\right)^2 - 2\frac{\mathrm{d}v}{\mathrm{d}x}\frac{\mathrm{d}\theta}{\mathrm{d}x} \\
b_z^M\,(x) &= -a_z\left(\frac{\mathrm{d}\theta}{\mathrm{d}x}\right)^2 - 2\frac{\mathrm{d}w}{\mathrm{d}x}\frac{\mathrm{d}\theta}{\mathrm{d}x} \\
b_\omega\,(x) &= \alpha_x\left(\frac{\mathrm{d}\theta}{\mathrm{d}x}\right)^2 \\
b_M\,(x) &= -\frac{\mathrm{d}^2w}{\mathrm{d}x^2}\frac{\mathrm{d}v}{\mathrm{d}x} + \frac{\mathrm{d}^2v}{\mathrm{d}x^2}\frac{\mathrm{d}w}{\mathrm{d}x} \\
b_y^T\,(x) &= a_z\theta\frac{\mathrm{d}\theta}{\mathrm{d}x} + 2\theta\frac{\mathrm{d}w}{\mathrm{d}x} \\
b_z^T\,(x) &= a_y\theta\frac{\mathrm{d}\theta}{\mathrm{d}x} - 2\theta\frac{\mathrm{d}v}{\mathrm{d}x}
\end{aligned} \tag{4.4}$$

with r_o, a_y, a_z being

$$r_o = \sqrt{\frac{J_y + J_z}{A} + (y_s)^2 + (z_s)^2} \tag{4.5}$$

$$a_y = \frac{1}{J_y} \int\limits_A z \left(z^2 + y^2\right) \mathrm{d}A - 2z_s$$

$$a_z = \frac{1}{J_z} \int\limits_A y \left(z^2 + y^2\right) \mathrm{d}A - 2y_s$$

while

$$\alpha_x = \frac{1}{I_\omega} \int\limits_A \left(z^2 + y^2\right) \omega\left(y, z\right) \mathrm{d}A \tag{4.6}$$

Note that $\widetilde{W}_y, \widetilde{W}_z$ vanish if the cross section is bisymmetric. These extra terms have been first derived by Zhang & Tong [7–9].

The passage from the spatial formulation in Eq. (2.1) to the one-dimensional form, see Eq. (4.1), needed additional approximations; the stresses other than $\sigma_o^{11}, \sigma_o^{12}, \sigma_o^{13}$ have been neglected and the terms involving the derivative $\partial u_1/\partial x_1$ have been discarded as smaller than other terms.

If the transverse and lateral loads are shifted along the y or z axes, as shown in Fig. 1, then the potential W_0 should be replaced by $\hat{W}_0$ extended by two terms, namely

$$\hat{W}_0 = W_0\left(v, w, \theta\right) + W_y\left(\theta\right) + W_z\left(\theta\right) \tag{4.7}$$

$$W_y\left(\theta\right) = \frac{e_1}{2} \int\limits_0^l q_y\left(x\right) \theta^2\left(x\right) \mathrm{d}x, \qquad W_z\left(\theta\right) = \frac{e_2}{2} \int\limits_0^l q_z\left(x\right) \theta^2\left(x\right) \mathrm{d}x \tag{4.8}$$

where $e_1 = y_1 - y_S e_2 = z_2 - z_S$ see Fig. 1. The derivation of the formulae (4.2)–(4.8) is here omitted, it will be published in a separate paper, see Czubacki & Lewiński [15].

The Rayleigh quotient method can be extended to the case when the bar's ends are stiffened by elastic plates which restrain the warping deformations on the faces: $x = 0$ and $x = l$. According to Eq. (7.130) in Petersen [6, Sec. 7.6.2] the warping stiffness of the end-plate equals

$$C_\omega = \frac{1}{3} G b \left(t_p\right)^3 h_s \tag{4.9}$$

where b represents the width of the plate, h_s – its height and t_p – its thickness; G is the shear modulus. The elastic energy stored in the end-plate at $x = 0$ equals, see Piotrowski & Szychowski [10–13].

$$W_\omega = \frac{1}{2} C_\omega \left(\left.\frac{\mathrm{d}\theta}{\mathrm{d}x}\right|_{x=0}\right)^2 \tag{4.10}$$

and the energy of the plate at the end $x = l$ is expressed similarly. The following non-dimensional coefficient will be used

$$K_\omega = \frac{lC_\omega}{2EI_\omega + lC_\omega} \tag{4.11}$$

to characterize the stiffness of the restraining end-plates, see Piotrowski & Szychowski [10–13].

The formulation (4.1) with the entities expressed by the formulae explained above makes it possible to solve practically all conceivable problems of stability of a straight bar, which will be illustrated in the sequel.

4.1. The axial buckling problem

Consider the problem of a bar subjected to compression by the forces P at both the ends; here $\sigma_o^{11} = -P/A$ and other stress components may be neglected. The problem of stability of equilibrium assumes the form of Eq. (4.1) where W is given by Eq. (9.5) in Lewiński & Czarnecki [1] while the potential W_0 reads

$$W_0 = \frac{1}{2}\int_0^l \left[\left(\frac{\mathrm{d}w}{\mathrm{d}x}\right)^2 + \left(\frac{\mathrm{d}v}{\mathrm{d}x}\right)^2 + 2z_s\frac{\mathrm{d}v}{\mathrm{d}x}\frac{\mathrm{d}\theta}{\mathrm{d}x} - 2y_s\frac{\mathrm{d}w}{\mathrm{d}x}\frac{\mathrm{d}\theta}{\mathrm{d}x} + (r_o)^2\left(\frac{\mathrm{d}\theta}{\mathrm{d}x}\right)^2\right]\mathrm{d}x \tag{4.12}$$

The formula above coincides with the corresponding formula known from Vlasov's theory of thin-walled bars of open cross sections, see e.g in Trahair et al [5] in Section 3.7.5 Eq. (3.57). This paves the way for computing the buckling loads of straight prismatic bars in tension irrespective of whether their profiles are thin-walled and open or not.

4.2. The lateral buckling problem

If the bar is subjected to two opposite bending moments at its ends the fields M_y^o and M_z^0 are constant and the shear forces T_z^o, T_y^o are zero. Then the stability problem can be elementary solved. In general, the shear forces are not zero, the bending moments depend on the variable x, which makes the problem far more difficult. In practice, only numerical methods are then applicable. The stability problem has the form (4.1) where W_0 can be, upon using the equilibrium equations, transformed to the form

$$W_0 = \frac{1}{2}\int_0^l \left[\frac{\mathrm{d}}{\mathrm{d}x}(a_y\theta - 2v)\frac{\mathrm{d}}{\mathrm{d}x}\left(\theta M_y^o\right) - \frac{\mathrm{d}}{\mathrm{d}x}(a_z\theta + 2w)\frac{\mathrm{d}}{\mathrm{d}x}\left(\theta M_z^o\right)\right]\mathrm{d}x + \widetilde{W}_y + \widetilde{W}_z \tag{4.13}$$

in which the shear forces are not present. The derivation of the above result will be published in the forthcoming paper by Czubacki and Lewiński [15]. The illustrative examples will concern mono- and bi-symmetric profiles; their parametrization is shown in Fig. 2.

4.2.1. A fork-supported bar loaded with q_z = const

Consider a bar with both ends fork-supported, restrained by the same end-plates at both the ends and loaded with $q_z = q$ = const of application points of coordinates $(x, 0, z_2)$ from $x = 0$ to $x = l$ (see Fig. 3).

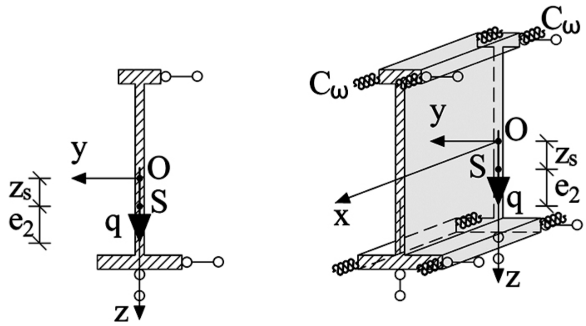

Fig. 2. Parametrization of the bar's mono-symmetric cross section; y and z are principal axes; position of the centroid (O) and the shear center (S). Possible point of application of the transverse load $q_z = q$ has coordinates: $(x, 0, z_2)$ $z_2 = e_2 + z_S$

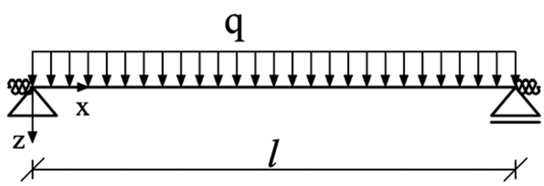

Fig. 3. A fork-supported bar restrained at both the ends, loaded with $q_z = q = \text{const}$

In the problem considered: $M_y^o = \frac{1}{2} q x (l - x)$, $q_y = 0$, $M_z^o = 0$; thus, according to (4.1) one obtains the rule for the critical value of the intensity of the transverse load

$$\frac{1}{|q_{\text{crit}}|} = \max_{\substack{\text{over } \theta, v \text{ being} \\ \text{kinematically} \\ \text{admissible}}} \frac{\int\limits_0^l \frac{\mathrm{d}}{\mathrm{d}x}\left(\frac{1}{2}a_y\theta - v\right)\frac{\mathrm{d}}{\mathrm{d}x}\left[x(l-x)\theta\right]\mathrm{d}x + \int\limits_0^l e_2\theta^2\mathrm{d}x - \int\limits_0^l \left(\frac{1}{2}a_y\right)\theta^2\mathrm{d}x}{\int\limits_0^l \left[EJ_z\left(\frac{\mathrm{d}^2 v}{\mathrm{d}x^2}\right)^2 + GJ\left(\frac{\mathrm{d}\theta}{\mathrm{d}x}\right)^2 + EI_\omega\left(\frac{\mathrm{d}^2\theta}{\mathrm{d}x^2}\right)^2\right]\mathrm{d}x + C_\omega\left(\left(\left.\frac{\mathrm{d}\theta}{\mathrm{d}x}\right|_{x=0}\right)^2 + \left(\left.\frac{\mathrm{d}\theta}{\mathrm{d}x}\right|_{x=l}\right)^2\right)} \tag{4.14}$$

where EJ_z is the bending stiffness, EI_ω is the warping stiffness due to torsion and GJ is the torsional stiffness.

Consider the simplest case of a bisymmetric profile (then $a_y = 0$), the case of $e_2 = 0$ and let the ends being not restrained, i.e. $C_\omega = 0$. Let us introduce

$$q_0 = \frac{1}{l^4}\sqrt{EJ_z \cdot EI_\omega}, \quad \xi = \frac{x}{l}, \quad \gamma = \frac{l^2 GJ}{EI_\omega}, \quad \theta = l\sqrt{\frac{EJ_z}{EI_\omega}}\phi, \quad v = l\psi \tag{4.15}$$

The functions $\phi(\xi)$, $\psi(\xi)$ are said to be kinematically admissible when they vanish at both ends of the bar: $\phi(0) = \phi(1) = 0$, $\psi(0) = \psi(1) = 0$. The critical load q_{crit} is expressed by

Eq. (4.1), which reduces now to the form

$$\frac{1}{\left|\frac{q_{crit}}{q_o}\right|} = \max_{\substack{\text{over } \phi,\, \psi \text{ being}\\ \text{kinematically}\\ \text{admissible}}} \frac{-\displaystyle\int_0^1 \frac{d\psi}{d\xi}\frac{d}{d\xi}\left[\xi\left(1-\xi\right)\phi\right] d\xi}{\displaystyle\int_0^1 \left[\left(\frac{d^2\psi}{d\xi^2}\right)^2 + \gamma\left(\frac{d\phi}{d\xi}\right)^2 + \left(\frac{d^2\phi}{d\xi^2}\right)^2\right] d\xi} \tag{4.16}$$

ready for further analytical or numerical treatments.

4.2.2. A fork-supported bar loaded with a point load acting at the middle of the bar

Consider a bar with both ends fork-supported and elastically restrained against warping, loaded with P acting at the middle of the bar at point $(l/2, 0, z_2)$ (see Figs. 1 and 4).

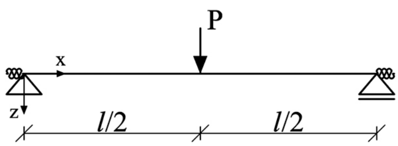

Fig. 4. The fork-supported bar, restrained at the ends, loaded with the load P acting at the middle of the bar

According to (4.1), (4.13) the critical load corresponding to the lateral-torsional buckling can be computed by solving the problem:

$$\frac{1}{|P_{crit}|} = \max_{\substack{\text{over } \theta, v \text{ being}\\ \text{kinematically}\\ \text{admissible}}} \frac{\displaystyle\int_0^{\frac{l}{2}} \frac{d}{dx}\left(\frac{1}{2}a_y\theta - v\right)\frac{d}{dx}\left(x\theta\right) dx + \int_{\frac{l}{2}}^{l} \frac{d}{dx}\left(\frac{1}{2}a_y\theta - v\right)\frac{d}{dx}\left[\left(l-x\right)\theta\right] dx + \left.\left(\left(e_2 - \frac{1}{2}a_y\right)\theta^2\right)\right|_{x=\frac{l}{2}}}{\displaystyle\int_0^l \left[EJ_z\left(\frac{d^2v}{dx^2}\right)^2 + GJ\left(\frac{d\theta}{dx}\right)^2 + EI_\omega\left(\frac{d^2\theta}{dx^2}\right)^2\right] dx + C_\omega\left(\left(\left.\frac{d\theta}{dx}\right|_{x=0}\right)^2 + \left(\left.\frac{d\theta}{dx}\right|_{x=l}\right)^2\right)} \tag{4.17}$$

Consider the simplest case of a bisymmetric profile (then $a_y = 0$), the case of $e_2 = 0$ and let the ends being not restrained, i.e. $C_\omega = 0$. Let us introduce the referential force

$$P_0 = \frac{1}{l^3}\sqrt{EJ_z \cdot EI_\omega} \tag{4.18}$$

The formula for the critical load P_{crit} given by (4.17) reduces now to the form

$$\frac{1}{\left|\frac{P_{crit}}{P_0}\right|} = \max_{\substack{\phi,\, \psi \text{ being}\\ \text{kinematically}\\ \text{admissible}}} \frac{-\displaystyle\int_0^{\frac{1}{2}} \frac{d\psi}{d\xi}\frac{d}{d\xi}\left(\xi\phi\right) d\xi - \int_{\frac{1}{2}}^{1} \frac{d\psi}{d\xi}\frac{d}{d\xi}\left[\left(1-\xi\right)\phi\right] d\xi}{\displaystyle\int_0^1 \left[\left(\frac{d^2\psi}{d\xi^2}\right)^2 + \gamma\left(\frac{d\phi}{d\xi}\right)^2 + \left(\frac{d^2\phi}{d\xi^2}\right)^2\right] d\xi} \tag{4.19}$$

ready for further analytical or numerical treatments.

5. A numerical method of maximizing the Rayleigh quotient

The Rayleigh quotient problem (4.1) will be solved numerically. The functions v, w, θ will be expanded by (truncated) series of orthogonal functions fulfilling the kinematic boundary conditions. To find the maximum value of the quotient (4.1) the numerical maximization algorithm can be used, or alternatively, the problem can be rearranged to a generalized eigenvalue problem of linear algebra.

The critical loads q_{crit}, P_{crit} given by formulae (4.14), (4.17) will be computed by the *Mathematica* software. The functions $\theta(x)$, $v(x)$ are expanded as follows:

$$v(x) = \sum_{i=1,3,5}^{n} A_i \sin\left(i\pi\frac{x}{l}\right), \qquad \theta(x) = \sum_{i=1,3,5}^{n} B_i \sin\left(i\pi\frac{x}{l}\right), \qquad A_i, B_i \text{ – unknowns} \tag{5.1}$$

In Table 1 and Table 2 the critical moments $M_{\text{cr}} = q_{\text{crit}} l^2/8$, $M_{\text{cr}} = P_{\text{crit}} l/4$ are set up respectively, where q_{crit}, P_{crit} are found numerically.

Table 1. Results concerning the problem of Fig. 3. Comparison of critical moments computed by (4.14) and by LTBeamN

Cross-section	K_ω	e_2 (m)	M_{cr} (kN·m)		
			LTBeamN	**Rayleigh quotient**	**(%)**
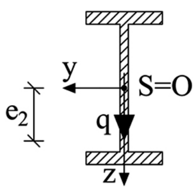	0	–0.25	239.01	238.97	0.02
		0	316.26	316.24	0.01
		0.25	418.25	418.17	0.02
	0.25	–0.25	252.21	252.36	–0.06
		0	329.72	329.80	–0.02
		0.25	430.56	430.67	–0.03
	0.5	–0.25	273.48	273.78	–0.11
		0	351.15	351.36	–0.06
		0.25	450.37	450.61	–0.05
	0.75	–0.25	313.46	314.81	–0.43
		0	391.05	392.35	–0.33
		0.25	487.57	488.73	–0.24
	1	–0.25	418.76	422.78	–0.96
		0	495.20	499.06	–0.78
		0.25	585.28	588.98	–0.63

Continued on next page

Table 1 – *Continued from previous page*

Cross-section	K_ω	e_2 (m)	M_{cr} (kN·m)		
			LTBeamN	**Rayleigh quotient**	(%)
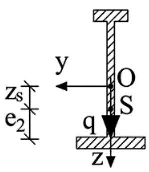	0	–0.2621	113.57	113.57	0.00
		0	156.20	156.20	0.00
		0.0379	163.81	163.81	0.00
	0.25	–0.2621	114.51	114.53	–0.02
		0	157.05	157.06	–0.01
		0.0379	164.62	164.64	–0.01
	0.5	–0.2621	116.17	116.19	–0.02
		0	158.52	158.55	–0.02
		0.0379	166.05	166.07	–0.01
	0.75	–0.2621	119.82	119.95	–0.11
		0	161.77	161.89	–0.07
		0.0379	169.17	169.29	–0.07
	1	–0.2621	134.48	135.26	–0.58
		0	174.50	175.16	–0.38
		0.0379	181.42	182.04	–0.34

Table 2. Results concerning the problem of Fig. 4. Comparison of critical moments computed by (4.17) and by LTBeamN

Cross-section	K_ω	e_2(m)	M_{cr} (kN·m)		
			LTBeamN	**Rayleigh quotient**	(%)
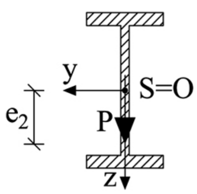	0	–0.25	269.61	269.61	0.00
		0	380.89	380.69	0.05
		0.25	533.83	534.36	–0.10
	0.25	–0.25	283.85	283.89	–0.01
		0	396.10	396.50	–0.10
		0.25	549.91	550.55	–0.12

Continued on next page

Table 2 – *Continued from previous page*

Cross-section	K_ω	e_2(m)	M_{cr} (kN·m)		
			LTBeamN	**Rayleigh quotient**	**(%)**
	0.5	–0.25	306.31	306.54	–0.08
		0	421.19	421.51	–0.08
		0.25	576.21	576.22	0.00
	0.75	–0.25	348.01	349.31	–0.37
		0	467.05	468.68	–0.35
		0.25	624.11	625.35	–0.20
	1	–0.25	453.80	458.20	–0.97
		0	584.79	588.86	–0.70
		0.25	748.93	753.16	–0.56
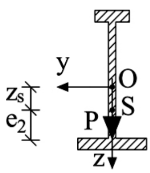	0	–0.2621	125.70	125.76	–0.05
		0	193.00	193.08	–0.04
		0.0379	206.08	206.14	–0.03
	0.25	–0.2621	126.56	126.59	–0.02
		0	194.04	194.05	–0.01
		0.0379	207.06	207.14	–0.04
	0.5	–0.2621	127.98	128.01	–0.02
		0	195.75	195.74	0.01
		0.0379	208.77	208.84	–0.03
	0.75	–0.2621	131.18	131.30	–0.09
		0	199.41	199.55	–0.07
		0.0379	212.55	212.71	–0.08
	1	–0.2621	143.99	144.71	–0.50
		0	213.98	214.75	–0.36
		0.0379	227.37	228.09	–0.32

The analysis is applied to the symmetrical beam section IPE500 ($I_z = 2141.7$ cm^4, $I_T = 89.006$ cm^4, $I_\omega = 1254300$ cm^6) and to the mono-symmetrical beam section DIM 300×200 M ($I_z = 1479,4$ cm^4, $I_T = 65.91$ cm^4 $I_\omega = 105563$ cm^6, $a_y = -20.32$ cm having the span length of $l = 8$ m and made by material of moduli: $E = 210$ GPa, $G = 81$ GPa. The results obtained by the chosen truncated series, are compared with the results obtained by the shareware program LTBeamN v 1.0.3, which is a newer version of the program LTBeam [16]. It is worth noting that the value of K_ω affects the speed of convergence of the method. To achieve a uniform accuracy the number of terms n has been appropriately correlated with K_ω. For $K_\omega = 0, 0.25, 0.5, 0.75, 1$ we choose $n = 11, 11, 40, 40, 80$ respectively. The differences between the results found by LTBeamN and those predicted by the method proposed are less than 1‰, cf Tables 1, 2.

6. Conclusions

The proposed method of assessing the values of the critical loads makes it possible to re-derive all the standard formulae for the critical axial forces (e.g. Euler's formula) and critical bending moments (Timoshenko's and Vlasov's formulae). It is worth stressing that all these formulae can be derived for bars of non-standard shape of cross sections, even multi-connected, since the assumptions of the Vlasov theory are here replaced by general Saint Venant solutions. Moreover, incorporation of elastic restraints against warping at the bar ends is possible.

Our study was based on the linearized elastic stability formulation. Possible extensions towards nonlinear stability analysis of bisymmeric thin-walled beams have been proposed in the recent papers by Giżejowski et al. [17, 18].

Acknowledgements

A part of this work was prepared within the Research Grant no 2019/33/B/ST8/00325 financed by the National Science Centre (Poland). Moreover, the authors express their thanks to Dr. hab. Andrzej Jan Szychowski for his constructive comments which have essentially contributed to the final form of the present paper.

References

[1] T. Lewiński and S. Czarnecki, "On incorporating warping effects due to transverse shear and torsion into the theories of straight elastic bars", *Acta Mechanica*, vol. 232, pp. 247–282, 2021, DOI: 10.1007/s00707-020-02849-7.

[2] A. Gawęcki, *Mechanics of Materials and Bar Structures*. Poznań: Wydawnictwo Politechniki Poznańskiej, 2003 (in Polish).

[3] S. Weiss and M. Giżejowski, *Stability of Metal Structures*. Warszawa: Arkady, 1991 (in Polish).

[4] S.P. Timoshenko and J.M. Gere, *Theory of Elastic Stability*. New York: Dover Publications, 1985.

[5] N.S. Trahair, M.A. Bradford, D.A. Nethercot, and L. Gardner, *The Behaviour and Design of Steel Structures to EC3*. London and New York: Taylor & Francis, 2008.

[6] Ch. Petersen, *Statik und Stabilität der Baukonstuktionen*. Braunschweig-Wiesbaden: Friedr. Vieweg & Sohn, 1982.

[7] L. Zhang and G.S. Tong, "Flexural-torsional buckling of thin-walled beam members based on shell buckling theory", *Thin-Walled Structures*, vol. 42, no. 12, pp. 1665–1687, 2004, DOI: 10.1016/j.tws.2004.05.004.

[8] L. Zhang and G.S. Tong, "Elastic flexural-torsional buckling of thin-walled cantilevers", *Thin-Walled Structures*, vol. 46, pp. 27–37, 2008, DOI:10.1016/j.tws.2007.08.011.

[9] G.S. Tong and L. Zhang, “Closure to “Elastic flexural–torsional buckling of thin-walled cantilevers” by Lei Zhang and Geng Shu Tong [Thin-Walled Structures 46(1) (2008) 27–37], *Thin-Walled Structures*, vol. 48, no. 2, pp. 187–190, 2010, DOI: 10.1016/j.tws.2009.10.006.

[10] R. Piotrowski and A. Szychowski, “Lateral-torsional buckling of beams elastically restrained against warping at supports”, *Archives of Civil Engineering*, vol. 61, no. 4, pp. 155–174, 2015, DOI: 10.1515/ace-2015-0042.

[11] R. Piotrowski and A. Szychowski, “Lateral torsional buckling of steel beams elastically restrained at the support nodes”, *Applied Sciences*, vol. 9, no. 9, art. no. 1944, 2019, DOI: 10.3390/app9091944.

[12] A. Szychowski, “A theoretical analysis of the local buckling in thin-walled bars with open cross-section subjected to warping torsion”, *Thin-Walled Structures,* vol. 76, pp. 42–55, 2014, DOI: 10.1016/j.tws.2013.11.002.

[13] A. Szychowski, “Stability of cantilever walls of steel thin-walled bars with open cross-section”, *Thin-Walled Structures,* vol. 94, pp. 348–358, 2015, DOI: 10.1016/j.tws.2015.04.029.

[14] K. Washizu, *Variational Methods in Elasticity and Plasticity,* 3rd ed. New York: Pergamon Press, 1982, DOI: 10.1002/zamm.19840640121.

[15] R. Czubacki and T. Lewiński, “On stability problems of straight elastic bars”, *in preparation*.

[16] Y. Galéa, “Moment critique de déversement élastique de poutres ?échies. Présentation du logiciel LTBEAM”, *Revue Construction Métallique. CTICM*, no. 2, 2003.

[17] M. Giżejowski, A. Barszcz, and P. Wiedro, “Refined energy method for the elastic flexural-torsional buckling of steel H-section beam-columns. Part I: Formulation and solution”, *Archives of Civil Engineering*, vol. 69, no. 1, pp. 513–537, 2023, DOI: 10.24425/ace.2023.144186.

[18] M. Giżejowski, A. Barszcz, and P. Wiedro, “Refined energy method for the elastic flexural-torsional buckling of steel H-section beam-columns. Part II: Comparison and verification for elements LTU and LTR”, *Archives of Civil Engineering*, vol. 69, no. 2, pp. 265–289, 2023, DOI: 10.24425/ace.2023.145267.

Zastosowanie metody ilorazu rayleigha do analizy stateczności sprężystych prętów prostych

Słowa kluczowe: pręty cienkościenne, stateczność, teoria prętów, wyboczenie giętno-skrętne

Streszczenie:

W pracy korzystamy z faktu, że teoria Własowa prętów cienkościennych o przekrojach otwartych została rozszerzona do postaci teorii typu Własowa odnoszącej się do praktycznie dowolnych kształtów profili pod warunkiem, że profile te nie doznają dystorsji poprzecznych przy typowych obciążeniach pręta. Struktura matematyczna modelu typu Własowa jest zgodna z oryginalnym modelem Własowa, natomiast charakterystyki przekrojowe są obliczane za pomocą innych formuł, które wymagają uprzedniego rozwiązania trzech pomocniczych zadań eliptycznych na obszarze określonym przez przekrój poprzeczny pręta. Ponadto zupełnie inne są wtedy formuły obliczania składowych stanu naprężenia na podstawie rozwiązań w ramach opisu jednowymiarowego, czyli całkowicie inny jest tzw. postprocessing tej metody. Matematyczna analogia między dwoma modelami teorio-prętowymi: Własowa i typu Własowa otwiera drogę do konstruktywnego rozwiązywania zadań stateczności: opisu wyboczenia giętno-skrętnego, wyboczenia od obciążeń skrętnych oraz zwichrzenia przy różnych możliwych warunkach brzegowych. Znane zadania stateczności prętów cienkościennych o przekrojach otwartych mogą być teraz uogólnione na przypadek prętów o dowolnych przekrojach zwartych, także niejednospójnych. Szczególnego znaczenia nabiera tu metoda maksymalizacji ilorazu Rayleigha, gdyż maksimum jest brane po trzech polach jednowymiarowych (dwa pola przemieszczeń i pole rozkładu kąta skręcenia), które spełniają warunki kinematyczne, są więc niezależne od nieznanego obciążenia krytycznego. Podkreślmy, że właśnie w tym tkwi istota metody ilorazu Rayleigha. W pracy podane są jawne postacie ilorazów Rayleigha

odnoszące się do wybranych postaci obciążeń. Formuły te mają postać podobną do formuł z publikacji: L. Zhang, G.S. Tong, “Flexural-torsional buckling of thin-walled beam members based on shell buckling theory”, Thin-Walled Structures, vol. 42, pp. 1665–1687, 2004, dotyczącej teorii prętów Własowa o przekroju otwartym. Podane są metody maksymalizacji ilorazów Rayleigha zapewniające dowolnie wysoką dokładność wyników. Opracowana metoda dotyczy dowolnych warunków podparcia, jednakże porównania przeprowadzono w przypadku standardowych zadań stateczności prętów podpartych widełkowo (z blachami czołowymi które wprowadzają więzy dotyczące spaczenia od skręcania), których wyniki są znane i akceptowane.

Received: 2024-02-20, Revised: 2024-03-29